Electronic Materials Letters, Vol. 2, No. 2 (2006), pp. 101-105

Electron Emission Reliability of Carbon Nanotube Paste and the Diode Emission Characteristics for a Microwave Power Amplifier

Jae-Hee Han[1], Jae Hong Park[1], A. S. Berdinsky[1], P. S. Alegaonkar[1], Ji-Beom Yoo[1,*], Hae Jin Kim[2], Jin Joo Choi[2], Joong-Woo Nam[3], and Chun Kyu Lee[3]

[1]Center for Nanotubes and Nanostructured Composites, Sungkyunkwan University, 300, Chunchun-Dong, Jangan-Gu, Suwon 440-746, Korea
[2]Department of Radio Science and Engineering, Kwangwoon University, 447-1, Wolgye-dong Nowon-Gu, Seoul 139-701, Korea
[3]Technology Development 3, Corporate R&D Center, Samsung SDI, 428-5, Gongse-Ri, Kiheung-Eup, Yongin 449-902, Korea

The field emission (FE) properties of carbon nanotube (CNT) paste on a cathode with a curved surface are reported in terms of its application in a traveling wave tube-microwave power amplifier (TWT-MPA). Initially, a stable and uniform emission current from the activated CNT paste emitter was obtained, during multiple trial of FE cycling (>80 mA/cm^2 at 3.5 V/μm). In addition, the effective electrical aging conditions (aging time and current) were investigated in an attempt to improve the emission reliability of the CNT emitters. After electrical aging, a gridded CNT cathode structure was fabricated, and the diode FE characteristics with the common ground configurations in anode and gate were investigated.

Keywords: carbon nanotube paste, field emission, traveling wave tube, micro power amplifier

1. INTRODUCTION

Thermionic cathodes used in high-power microwave tubes are a source of many technical difficulties due to their limitations regarding their current density, their high-temperature operation and associated tube design restrictions. Alternative types of cathodes without these technical limitations and with lower manufacturing costs have therefore long been sought. Field emitter arrays (FEAs) have various advantages such as an instantaneous power-up, that results in high pulse repetition frequencies (>10 GHz), and low operating and switching voltages when utilized as cold cathodes in microwave power amplifiers (MPAs)[1-6]. In traveling wave tubes (TWTs), they can permit a size reduction as the emitted electron beam is gated at the source, eliminating the need for a prebunching section. Spindt-type FEA cathodes have been developed for more than several decades [7-9]. Although at least one such cathode with an approximate area of 1 mm^2 was used to generate a 90 mA beam in a TWT [9], the lifetime of this type cathode and its ability to scale its size to areas of 10 to 100 cm^2 are of concern. In addition, a conventional fabrication process for a Spindt-type FEA requires the use of expensive and complicated semiconductor technologies.

Based on this study's calculations to characterize a gridded CNT cathode in this present TWT using 1-D LMSuite simulation, it was found that the gain is 15 dB in the frequency range of 8-12 GHz (X-band) if the anode current is 10 mA and the input power is 100 mW [10]. In this report, the field emission (FE) properties of the carbon nanotube (CNT) paste on a cathode with a curved surface for a TWT-MPA are presented. In addition, the diode FE characteristics with the common ground configuration in anode and gate are measured.

2. EXPERIMENTAL

The CNT paste was prepared using a mixture of multi-walled CNTs powders synthesized through a chemical vapor deposition method, organic vehicles, and inorganic binders. Spin on glass (SOG) as an inorganic binder and additive to the CNT paste were utilized. Details are described in a previous report by the authors[11]. Initially, to investigate the FE properties of the CNT pastes, the CNT paste was screen-printed onto an indium tin oxide (ITO)-coated glass substrate, and activated (i.e., the buried CNTs on surface were protruded) by adhesive tape, then transferred into a vacuum

*Corresponding author: jbyoo@skku.ac.kr

chamber (~3×10^{-6} Torr) and direct current (dc) voltage was applied. For the anode, a flat stainless steel (SUS) plate was used. The emission area was ~1×1 cm^2 and the distance between the cathode and SUS anode was fixed at 200 μm.

To fabricate a CNT-based FEA cathode, following the CNT paste synthesis the paste was rubbed over a round cathode (diameter, d ~ 4.3 mm) with a curved surface (a radius of curvature, r ~ 9.7 mm) designed specifically for the X-band (8 - 12 GHz) TWT-MPA.

For an analysis of the surface morphology of the CNTs field-emission scanning-electron microscopy (FESEM, JSM6700F) was utilized. An energy-dispersive X-ray spectrometer (EDS) was employed for an elemental analysis.

3. RESULTS AND DISCUSSION

It is well understood that the as-prepared CNT emitters show poor emission characteristics due to the insufficient CNT emitter density at the film surface. A special surface treatment, termed an the activation treatment, is required in order to cause the CNT emitters to protrude on the surface. A considerable amount of work related to the activation treatment has been carried out, such as adhesive taping, soft rubber rolling, laser treatment and irradiation with energetic ions [12-15]. However, the adhesive tape technique is a convenient and well-suited candidate for causing the buried CNTs to protrude. In this work this technique was adopted.

The FE characteristics of an activated CNT emitter are shown in Fig. 1. Multiple FE cycling was carried out in order to obtain a stable and uniform emission current from the activated CNT emitters. The turn-on electric field, E_{to}, can be defined as the electric field necessary to obtain a current density of ~10 μA/cm^2. The E_{to} of the CNT emitter was recorded as ~1.8 V/μm and an emission current density of ~80 mA/cm^2 was obtained at an applied electric field of 3.5 V/μm.

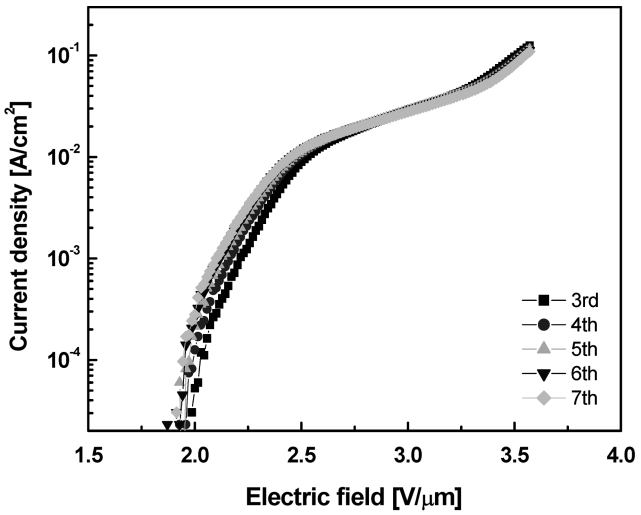

Fig. 1. Recorded I-V characteristics for the activated CNT paste emitter.

To be incorporated into actual devices, the emission characteristics of the CNT paste emitters should be stable at their operational condition over a long period of time. The stability and reliability of the CNT emitters was found to be strongly dependent on the vacuum level and residual gas[16,17]. Gradual degradation and abrupt failure of single-walled CNTs (SWNTs) and multi-walled CNTs (MWNTs) during FE have been reported in *in-situ* observation[18-20]. It is expected that coating with wide band gap materials and post-treatment can enhance the environmental stability and reliability of the CNT emitter [17,21]. In present work, the effective electrical aging conditions were investigated in an attempt to improve the emission reliability of the CNT emitters.

CNT emitters prepared by a screen-printing of the CNT paste were electrically treated in a high vacuum chamber

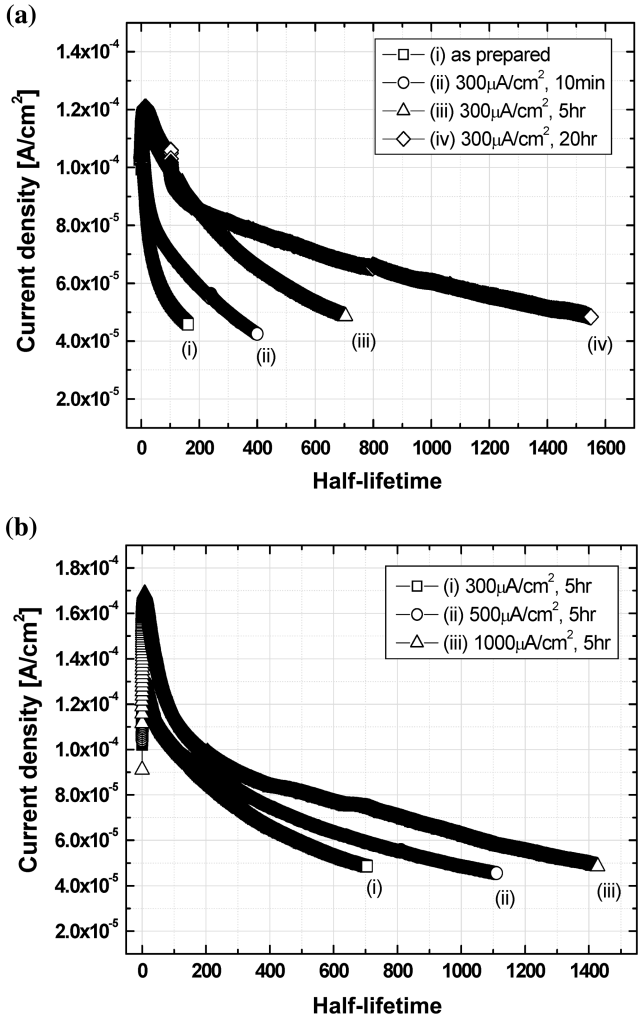

Fig. 2. The plot of the emission current density vs. the half-lifetime of the CNT emitters according to the aging time (a) and the aging current density (b).

with a parallel diode-type configuration as stated in the Experimental section. A pulsed voltage supply (duty cycle 1/1000) was coupled to the system. In order to evaluate the reliability of a CNT emitter, the half-lifetime of the CNT emitters depending on the electrical aging conditions were measured. The half-lifetime of CNT emitter can be defined as the time to needed to decrease the current density to half of its initial value. Figure 2(a) shows half-lifetime of CNT emitters as a function of the electrical aging time. For the as-prepared sample, the half-lifetime was found to be ~121 hr. The emission current density rapidly decreased during the initial stage of the half-lifetime measurement. As time progressed, the the current degradation was gradually reduced with a subsequent degradation rate of current density from 1.2 to 0.125 $\mu A/cm^2$ per hour.

After the electrical aging, the CNT emitters showed a longer half-lifetime. As the aging time increased from 10 min to 20 hr, the half-lifetime of the CNT emitters increased from approximately 300 to 1500 hr. This improved half-lifetime can be attributed to the removal of the weaker and extremely sharp CNTs from their local positions.

Figure 2(b) shows the half-lifetime of the CNT emitters as a function of the aging current. The current density for the electrical aging was varied from 300 to 1000 $\mu A/cm^2$ by controlling the pulse dc voltage applied to an anode plate. It was observed that as the aging current density increases from ~300 to ~1000 $\mu A/cm^2$, the half-lifetime of the CNT emitters increases from ~670 to ~1378 hr. The results reveal that the reliability of the CNT emitters can be improved by a long-term electrical conditioning and that the passage of a higher current density can effectively reduce the aging time.

Figure 3 shows the recorded photographs for the (a) anode, (b) cathode, and (c) assembly of the X-band TWT-MPA, respectively. The arrows in Figs. 3(a) and 3(b) indicate an anode hole through which the emitted electrons from the cathode pass, and a gridded Ni cathode (having a concave surface for electron focusing with a radius of curvature ~9.7 mm), where the CNT paste film is coated. For the gridded cathode, a concave-down molybdenum (Mo) mesh grid (transparency of 72%) with an identical radius of curvature

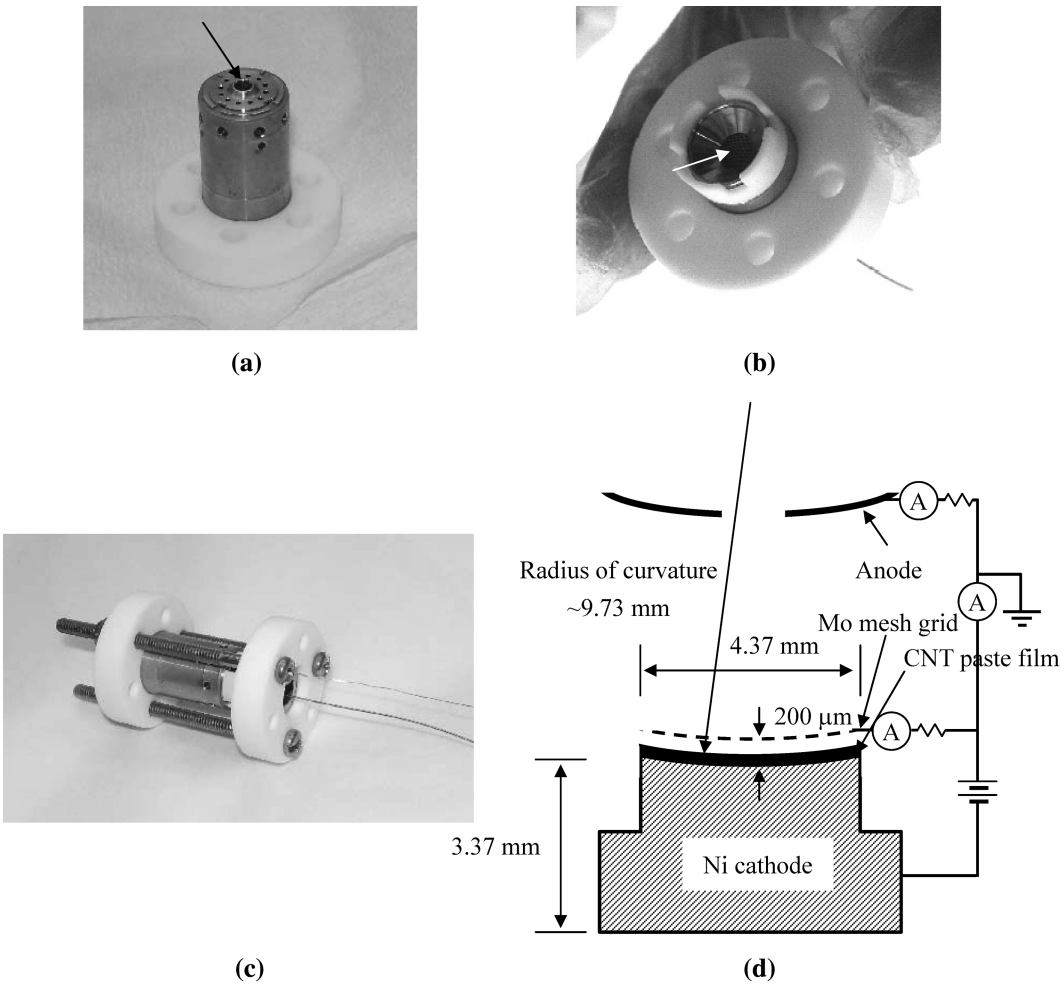

Fig. 3. Photographs of the (a) anode, (b) cathode, and (c) the assembly for the X-band TWT-MPA. (d) schematic depiction for the gridded assembly. The anode and grid are common and grounded. Negative potential is applied to the cathode.

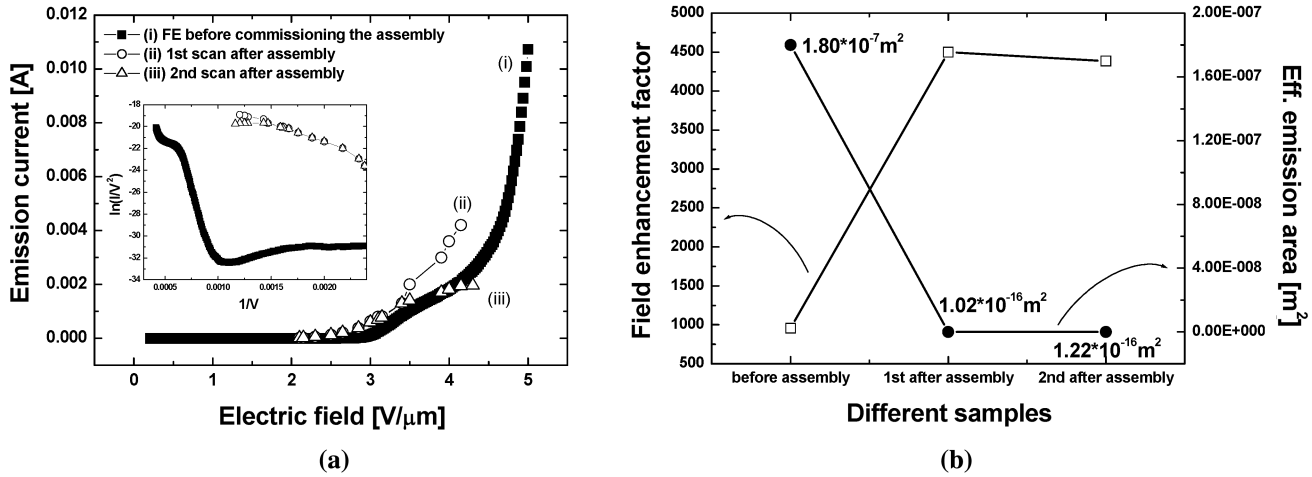

Fig. 4. (a) Recorded *I–V* characteristics for (i) before commissioning the CNT cathode assembly and (ii-iii) 1st & 2nd scan after commissioning the assembly. (b) corresponding plots for γ and *A*.

as that of the Ni cathode was designed and attached to the cathode in order to maintain a grid–cathode gap distance of 200 μm. Figure 3(d) shows the schematic layout for this assembly. The anode and grid were commonly grounded, and negative potential was applied to the cathode.

Figure 4 shows the *I–V* characteristics before and after the assembly. From Fig. 4(a), it appears that the first *I–V* scan of the assembly is nearly identical to that of the assembly that was commissioned. The FE current saturation occurs in the last part of the second scan, which makes it closer to the one before the commissioning of the assembly. To investigate this issue, the field enhancement factor, γ, and the effective emission area, *A*, from the *I–V* relationship according to the FN model [18] was calculated as;

$$I = A\frac{1.5\times10^{-6}}{\phi}\left(\frac{V}{d}\right)^2\gamma^2 exp\left(\frac{10.4}{\sqrt{\phi}}\right)exp\left(\frac{-6.44\times10^{9}\phi^{1.5}d}{\gamma V}\right) \quad (1)$$

where *A* has the dimension of the area [m^2] to the first approximation, indicates the emitting area. The work function ϕ is in eV (assuming 5 eV for the CNT emitter). The field enhancement factor, γ, as a dimensionless entity, is defined as $F = \gamma V/d$, where *F* is the local field at the emitter surface [V/m] and *d* is the interelectrode distance. γ and *A* can be calculated from the slope (*m*) of the FN plot [$\ln(\frac{I}{V^2}) = \ln b + \frac{m}{V}$), where ln *b* is the ordinate in the FN plot]. Figure 4(b) shows the plot of γ and *A* according to the different *I–V* scans before and after the commissioning of the assembly. The field enhancement factor, γ, increased from 956 (before the commissioning of the assembly) to 4498 (for the first scan after commissioning). However, the corresponding effective emission area, *A*, decreased significantly from 1.80×10^{-7} to 1.02×10^{-16} m^2. This most probably implies that there were numerous effective CNT emitters that participated in the FE before the commissioning of the assembly, correspondingly causing a high population density, thus causing a reduction in the field enhancement factor, γ, due to *the screening effect*. However, the emission site density greatly decreased for the first scan after the commissioning of the assembly, resulting in an increment of γ. It is likely that a handling process, for example, laser brazing, while commissioning the assembly, would deteriorate the CNT film quality on the cathode. For the second scan after the commissioning of the assembly, γ slightly decreased to be 4385 and *A* increased to be 1.22×10^{-16} m^2, compared to the 1st scan. It is possibly that the most dominant CNT emitters disappeared after the first scan, thus the next candidates with a higher population could play the role of increasing *A* and decreasing γ in the FE.

4. CONCLUSION

In this article, the FE characteristics of an activated CNT paste emitter were investigated, in particular the electrical aging effect on emission reliability, and a gridded CNT cathode structure was fabricated for a designed TWT-MPA. Stable and uniform emission currents were obtained from the CNT paste during a multiple FE cycling (>80 mA/cm^2 at 3.5 V/μm) procedure. Additionally, investigations on the effective electrical aging conditions (aging time and current) were carried out in an attempt to improve the emission reliability of the CNT emitters. It is suggested that the reliability of CNT emitters can be improved through the long-term electrical conditioning, and that a higher current density can effectively reduce the aging time. For the gridded CNT cathode structure, diode-type FE characterizations were performed with a common ground configuration for the anode and the gate.

REFERENCE

1. F. M. Charbonnier, J. P. Barbour, L. F. Garrett, and W. P. Dyke, *Proc. IEEE* **51**, 991 (1963).
2. F. Charbonnier, *Appl. Surf. Sci*. **94/95**, 26 (1996).
3. A. V. Haeff, *Electron* **12**, 30 (1939).
4. A. V. Haeff and L. S. Nergaard, *Proc. IRE* **28**, 126 (1940).
5. R. I. Sarbacher and W. A. Edson, *Hyper and Ultrahigh Engineering*, New York, NY: Wiley (1943).
6. A. J. Lichtenberg, *IRE Trans. Electron Devices* **ED-9**, 345 (1962).
7. K. L. Jensen, *Phys. Plasmas* **6**, 2241 (1999).
8. F. M. Charbonnier, J. P. Barbour, L. F. Garrett, and W. P. Dyke, *Proc. IEEE* **51**, 991 (1963).
9. D. R. Whaley, B. M. Gannon, C. R. Smith, C. M. Armstrong, and C. A. Spindt, *IEEE Trans. Plasma Sci.* **28**, 727 (2000).
10. H. J. Kim and J. J. Choi (unpublished).
11. J. H. Park, J. S. Moon, J. H. Han, A. S. Berdinsky, J. B. Yoo, C. Y. Park, J. W. Nam, J. H. Park, C. G. Lee, and D. H. Choe, *J. Vac. Sci. Technol. B* **23**, 702 (2005).
12. T. J. Vink, M. Cillies, J. C. Kriege, and H. W. J. J. van de Laar, *Appl. Phys. Lett*. **83**, 3552 (2003).
13. Y. C. Kim, K. H. Sohn, Y. M. Cho, and E. H. Yoo, *Appl. Phys. Lett.* **84**, 5350 (2004).
14. W. Zhao, N. Kawakami, A. Sawada, and M. Takai, *J. Vac. Sci. Technol. B* **21,** 1734 (2003).
15. D. H. Kim, C. D. Kim, and H. R. Lee, *Carbon* **42**, 1807 (2004).
16. G. W. Ho, A. T. S. Wee, and J. Lin, *Appl. Phys. Lett.* **79**, 260 (2001).
17. W. K. Yi, T. W. Jeong, S. G. Yu, J. N. Heo, C. S. Lee, W. S. Kim, J. B. Yoo, and J. M. Kim, *Adv. Mater.* **14**, 1464 (2002).
18. J. M. Bornard and C. Klinke, *Phys. Rev. B* **67**, 115406 (2003).
19. Z. L. Wang, R. P. Gao, W. A. de Heer, and P. Poncharl, *Appl. Phys. Lett.* **80**, 856 (2002).
20. T. Fujieda, K. Hidaka, M. Hayashibara, T. Kamino, H. Matsumoto, Y. Ose, H. Abe, T. Shimizu, and H. Tokumoto, *Appl. Phys. Lett.* **85**, 5739 (2004).
21. W. S. Kim, J. H. Lee, T. W. Jeong, J. N. Heo, B. Y. Kong, Y. W. Jin, J. M. Kim, S. H. Cho, J. H. Park, and D. H. Choe, *Appl. Phys. Lett.* **87**, 163112 (2005).